Fluid Mechanics of the Dead Sea

Eckart Meiburg[1] and Nadav Lensky[2]

[1]Department of Mechanical Engineering
University of California Santa Barbara
Santa Barbara, CA 93110, USA
Email: meiburg@engineering.ucsb.edu
[2]Dead Sea Observatory
Geological Survey of Israel
and Institute of Earth Science
Hebrew University of Jerusalem
Jerusalem, Postal code, Israel
Email: nadavl@gsi.gov.il

Xxxx. Xxx. Xxx. Xxx. YYYY. AA:1–30

https://doi.org/10.1146/((please add article doi))

Keywords

hypersaline brine, supersaturation, buoyancy-driven flows with precipitation and dissolution, multiphase flow, double diffusion, thermohaline staircases, internal waves, salt deposits, lake level decline, beach formation, river incision, sediment transport

Abstract

The environmental setting of the Dead Sea combines several aspects whose interplay creates flow phenomena and transport processes that cannot be observed anywhere else on Earth. As a terminal lake with a rapidly declining surface level, the salinity of the Dead Sea is close to saturation, so that the buoyancy-driven flows common in lakes are coupled to precipitation and dissolution, and large amounts of salt are being deposited year-round. The Dead Sea is the only hypersaline lake deep enough to form a thermocline during summer, which gives rise to descending supersaturated salt fingers that precipitating halite particles. In contrast, during winter the entire supersaturated, well-mixed water column produces halite. The rapid lake level decline of $O(1m/yr)$ exposes vast areas of newly formed beach every year, which exhibits deep incisions from streams. Taken together, these phenomena provide insight into the enigmatic 'salt giants' observed in Earth's geological record, and offer lessons regarding the stability, erosion and protection of arid coastlines under sea level change.

Contents

1. INTRODUCTION

The Dead Sea is a terminal hypersaline lake located in the arid Jordan Rift Valley in the Eastern Mediterranean region of the Levant (fig. 1a, Wikipedia: Dead Sea). With a length of $50km$ and a width of $15km$, it has a salinity level nearly ten times that of the ocean, giving it a typical density of approximately $1.24g/cm^3$. This high salinity originated with salt water intrusions from the Mediterranean about 5 million years ago, and it subsequently increased due to the absence of an outlet to the lake, so that the surface level of the Dead Sea is governed by the balance between inflow and evaporation, which causes the salt to accumulate. Since the early 1960s, the construction of dams along the Jordan river and its tributaries has created an imbalance between inflow into the Dead Sea and evaporation from its surface. As a result, the lake level of the Dead Sea has been declining at a rate of about $1m/yr$ over the last 45 years, and its coastline has receded (fig. 1b, Lensky et al. 2005). The surface of the Dead Sea is currently (2024) located at approximately $438m$ below sea level, making it the lowest elevation on Earth. With a depth of $280m$, it is also the deepest hypersaline lake in the world.

The sea level decline over the last four decades has caused part of the Dead Sea's water column to become supersaturated for much of the year (Anati et al. 1987, Anati 1997, Lensky et al. 2005, Sirota et al 2016, Steinhorn 1983, Stiller et al. 1997). The resulting excess salinity precipitates and forms halite ($NaCl$) crystals that settle out, in a manner akin to 'marine snow,' thus forming a salt deposit on the lake floor that has already grown to a thickness of about $4m$ since its inception in the early 1980s (fig. 1c,d, Sirota et al. 2017). As a consequence of the high salinity, many of the gravity-driven flow phenomena familiar from other environmental settings, such as gravity currents, internal waves, plumes and double-diffusive salt fingers, are coupled to the formation and dissolution of halite and the formation and growth of salt deposits (figure 1c-f, Anati and Stiller 1991, Arnon et al. 2016, Ouillon et al. 2019, Sirota et al., 2020).

While many other deep hypersaline water bodies have given rise to large-scale salt precipitation during earlier geological periods (e.g., Hsu 1972, Roveri et al. 2014a), today the Dead Sea is the only deep lake on Earth displaying this phenomenon (Sirota et al. 2017,

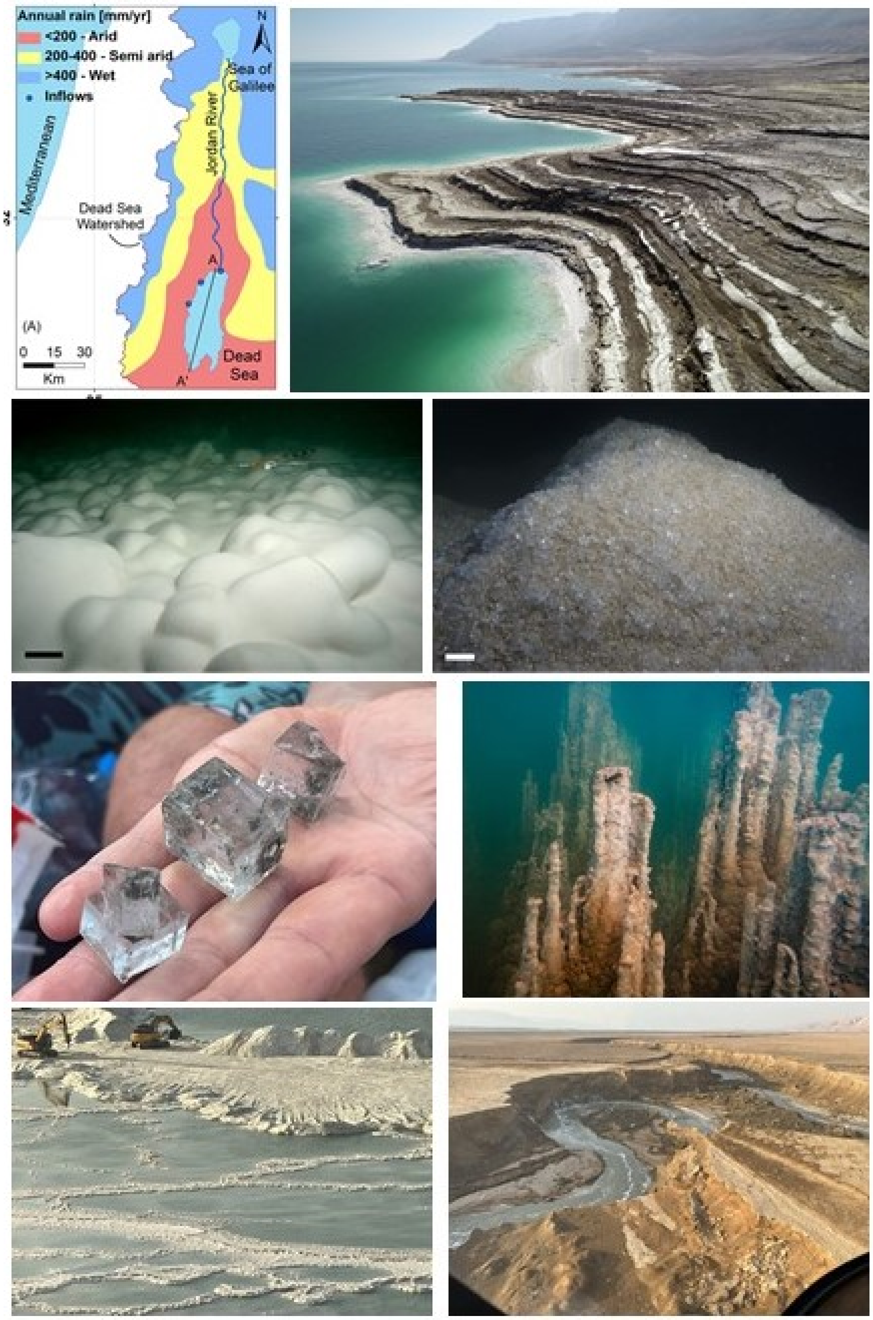

Figure 1

a) Dead Sea location map; b) Dead Sea coastline and beach, showing annual steps of $O(1m)$ due to lake level fall; c) Smooth salt deposit formed during winter, scale indicates $5cm$; d) Salt dome consisting of coarse crystals, scale indicates $5cm$; e) Cubic halite crystals formed during summer; f) Salt chimneys, which can range from a few cm to $20m$ in size; g) Industrial potassium extraction in the southern Dead Sea; h) Incision by Nahal Ha'Arava channel (c,d,f courtesy of Liran Ben Moshe).

2020, 2021). This renders it a unique environment for studying the flow processes governing the formation of so-called 'salt giants,' large-scale salt deposits in the Earth's crust that can be up to $O(1km)$ thick, and that are of considerable interest to geologists as well as the oil and gas industry (Warren 2010; Sirota et al. 2020). The processes forming these salt giants have been the focus of a longstanding debate (Schmalz, 1969; Hsu, 1972; Roveri et al., 2014a; Simon and Meijer, 2017), since global mass balance arguments alone cannot explain their observed spatial variations in thickness (Hsu, 1972; Meijer and Krijgsman, 2005). Hence the considerable regional and seasonal variations of the depositional processes, as a result of the prevailing hydroclimatology, have been an active research area in recent years. The precipitation of halite has furthermore resulted in the growth of unique features such as 'salt chimneys' (fig. 1f) that grow from the lake floor all the way to the surface of the Dead Sea, and 'salt domes,' (fig. 1d) whose emergence is not well understood at present (Sirota et al. 2017). Advancing our understanding of the physico-chemical transport processes in the Dead Sea is also essential in light of certain industrial applications, such as the extraction of potash and other minerals, both from the Dead Sea and other bodies of water around the world. The Dead Sea Works and Arab Potash at the southern end of the Dead Sea are among the largest such industrial operations, and our understanding of the effects they have on the natural environment of the Dead Sea is insufficient at present (fig. 1g). Here again, lessons learned from the Dead Sea will be of use for similar resource extraction projects around the world.

The surface temperature of the Dead Sea varies from $24°C$ in the winter to $37°C$ in the summer. During the winter, its water column is generally well-mixed, whereas during the summer it exhibits a pronounced stratification and a strong pycnocline, with warmer, saltier water near the surface (epilimnion) and cooler, less salty water below (hypolimnion). The thermo/halocline is typically located at a depth of about $25m$. As a result, double-diffusive salt fingering plays a prominent role in the Dead Sea. The circulation patterns in the Dead Sea are furthermore influenced by wind, Earth's rotation, and the density differences between the epi- and hypolimnion. During the summer Mediterranean sea breezes form in the afternoon, cross the water divide and usually reach the Dead Sea after sunset. They channel southward along the rift valley and form intense night winds that peak around midnight. These night winds enhance evaporation, thus cooling the surface and increasing its salinity, and they generate surface waves and currents that elevate the lake surface downwind. During the day the situation is somewhat reversed, although the winds are much less intense, and evaporation, wave action and current strength are reduced. As a consequence of this periodic forcing by the wind, the lake surface can exhibit standing waves known as seiches (Lensky et al. 2018, Arnon et al. 2019).

Its rapid lake level decline furthermore renders the Dead Sea a unique setting for studying the sediment transport processes governing the emergence and evolution of new beaches, since it preserves key features of these processes on the newly formed beaches (fig. 1b). The lake level decline has also had a strong effect on the morphodynamics of the streams entering the Dead Sea, in that it has drastically altered their slope, and hence their incision and meandering behavior, along with their sediment transport characteristics (fig. 1h, Ben Moshe et al. 2008, Dente et al. 2017, 2018, Eyal 2019). Hence, past and future observations from the Dead Sea will provide important lessons for a number of reservoirs and terminal lakes around the world that have been experiencing rapid lake level decline, such as Lake Powell and Lake Mead along the Colorado river in the U.S., or the Salton Sea in California's Imperial Valley. They also provide insight into past climates, when streams and coastlines experienced similar conditions during glacial/interglacial cycles as ocean levels declined by $O(100m)$ (Eyal et al., 2019, 2021). Many of the research questions outlined here are furthermore of general interest in the broader context of water resource management in arid regions on Earth, a topic of rapidly increasing importance. They also affect other environmental concerns such as the stability and erosion of coastlines, the resilience of engineering infrastructure and potential measures that can be taken to protect it, as well as desertification and the preservation of bird migration routes.

As a historical note, we remark that the first modern survey of the Dead Sea was conducted by the Geological Survey of Israel in 1959–60, and the report published (Neev and Emery, 1967) remains the baseline study for our understanding of the physical and chemical properties of the lake's water column. The lake was observed to be stratified, with a surface water density of $1.19g/cm^3$, a transition layer at $20-40m$, and an underlying main water body density of $1.23g/cm^3$. The results of even earlier density profiles are summarized by Oren (2015): two fatal expeditions by the Irish explorer Christopher Costigan (1835) and the British Lieutenant Thomas Molyneux (1847) preceded a successful expedition by the U.S. Navy Lieutenant William Francis Lynch (1801–1865). More detailed profiles were measured in 1864 by the French explorer Duc de Luynes, who reported density profiles qualitatively similar to those measured almost a hundred years later (Neev and Emeri 1967), but with a more dilute surface layer of $1.16g/cm^3$.

This article provides an overview of the fluid dynamical and associated sediment transport processes governing the Dead Sea. Section 2 reviews the key properties of the water column, along with their seasonal and regional variations. Section 3 focuses on the role of double-diffusive fingering during the summer months, which causes supersaturated descending salt fingers to emerge that precipitate halite. Section 4 reviews the properties of internal waves along the pycnocline, along with the role of Earth's rotation in generating such waves. Section 5 highlights the main features of the evolving salt deposits and their spatial variations. Section 6 reviews key aspects of the beach evolution under lake level decline, especially the formation of beach berms and the sorting of coarse sediments. Section 7 focuses on the incision and meandering behavior of seasonal rivers as the lake level declines. Section 8 highlights several open questions regarding the fluid dynamics and sediment transport processes shaping the Dead Sea, as well as the mechanisms governing the formation and evolution of the salt deposits. Finding answers to these questions will require additional field and laboratory investigations, along with computational efforts and the development of simplified models. Finally, section 9 summarizes the main observations to date and provides an outlook.

2. THERMOHALINE STRATIFICATION OF THE DEAD SEA

Several processes compete in setting up the thermohaline stratification of terminal lakes. While freshwater inflows dilute the salinity of the surface layer, evaporation results in a loss of freshwater, which tends to increase the surface salinity. Similarly, a temperature difference between the freshwater inflow and the body of the lake can stratify its temperature distribution, which in addition is affected by radiative heating from the sun as well as by evaporative heat loss. Finally, vertical mixing processes in the water column, for example due to the actions of wind and water waves, or as a result of fluid dynamical instabilities, play an important role in governing the thermohaline stratification of the water column. Seasonal and regional variations in these processes result in corresponding variations of the

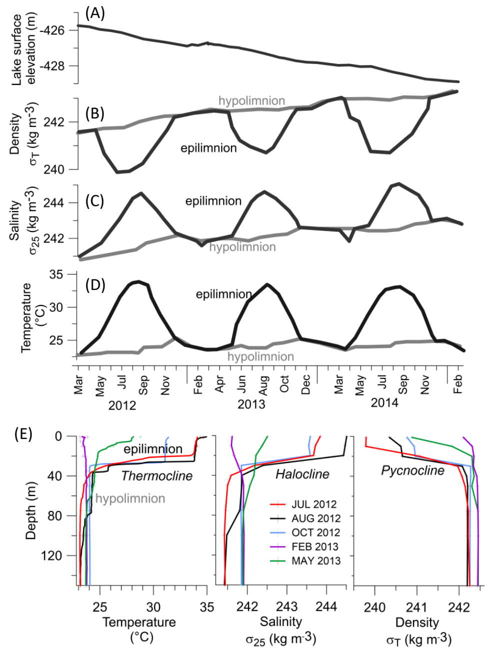

Figure 2

Evolution in time of the seasonal thermohaline stratification of the Dead Sea during 2012-2014: a) Lake level; b) Density of the epilimnion (measured at $10m$ depth) and hypolimnion (measured at $50m$ depth); c) Salinity (same depths); d) Temperature (same depths). Depth profiles of temperature, salinity and density are shown in frame e (modified after Arnon et al. 2019).

thermohaline stratification, with important consequences for the fluid flow and transport processes governing the Dead Sea. The dependence of the brine density on temperature and salinity is well established, so that the density stratification can be determined directly from the salinity and temperature distributions (Anati 1997; Gertman et al. 2010). We note that hypersaline lakes such as the Dead Sea are water bodies that reach the temperature-dependent solubility limit of salt at least during part of the year. In such lakes the dissolved salt, mostly halite ($NaCl$), can crystallize and sediment (Stiller et al. 1997, Sirota et al. 2016), which will have an additional influence on the effective density stratification of the water column.

Measurements in the Dead Sea dating back to 1864 (by Lartent and Bruck, as described in Oren 2015) showed the existence of a diluted epilimnion along with a year-round stable density stratification, rendering the lake meromictic, so that the entire water column never turned over. This situation changed during the late twentieth century as the negative water balance resulting from the partial diversion of the Jordan river led to an increase of the surface salinity. By the early 1980s the surface salinity reached the level of the underlying main water body, which enabled vertical convection to occur along the entire water column, so that the Dead Sea transitioned from a meromictic to a holomicic lake (Neev and Emery 1967, Steinhorn 1985). As a water body that had essentially been fossilized since earlier periods of lake level decline, the hypolimnion was nearly saturated with halite during the meromictic period, so that the transition to holomictic winter overturns resulted in the onset of halite precipitation. Since then the Dead Sea has experienced annual overturns during the winter months when the surface cools (Steinhorn et al. 1979; Anati et al. 1987), as well as halite precipitation (Steinhorn 1983). An unusual interlude developed from 1992 to 1995 (Stiller et al. 1984; Anati 1997; Gertman and Hecht 2002), when the density of the surface layer decreased significantly during the exceptionally rainy winters of 1991/92 and 1992/93 that resulted in high freshwater inflows and the dilution of the epilimnion, as well as a significant lake level rise of about $2m$ (Beyth et al. 1993). As a result, the water column did not overturn during those winters. These exceptional winters affected the entire southeastern Mediterranean region (Halpert et al. 1993; Genin et al. 1995), most likely due to lingering effects from the Mt. Pinatubo eruption. This review focuses on the dynamics of the Dead Sea during the holomictic period, when it became the only modern analogue in the world for studying the precipitation of halite in deep hypersaline lakes, which were common in dry climates throughout geological history (Warren 1999, Jackson and Hudec 2017).

Due to the stabilizing temperature distribution as a result of surface heating, today the Dead Sea is stably stratified throughout eight months of the warm season, despite the unstably stratified salinity field driven by evaporation (fig. 2). The stable summer stratification is most pronounced during mid July, when the epilimnion can be $12^{\circ}C$ warmer and $2.5kg/m^3$ less dense than the hypolimnion (Sirota et al., 2016). The transition layer (metalimnion) is typically centered at a depth of 20–$30m$ (Gertman and Hecht 2002; Arnon et al. 2016, fig. 2e). The stratification diminishes throughout the fall due to surface cooling. During winter the water column turns over, so that it becomes well-mixed for about four months. This winter convection is driven by the cooling of the surface water, as well as by salinity increase due to evaporation, and by wind-generated wave action. We note while $NaCl$ represents the main component of the brine, other dissolved ions are present as well, such as Mg, Ca and K. These exist in lower concentrations, so that they do not precipitate and instead their concentration continues to increase. In turn, this increases the solubility of $NaCl$, with the combined net effect being a long term density increase of the Dead Sea at a rate of approximately $0.25kg/(m^3yr)$ (fig. 2b, Gertman and Hecht 2002, Arnon et al. 2016, Sirota et al. 2016, 2017).

After having established the key properties of the water column, we will now discuss the transport mechanisms governing the spatio-temporal evolution of the salinity and temperature fields, with a particular focus on the exchange of heat and salt between the epi- and hypolimnion.

3. DOUBLE DIFFUSION

In the following we discuss the role of double-diffusive instabilities for the transport of salt and heat in the Dead Sea. Initially we will focus on base states that depend on the vertical direction only. Subsequently, we will discuss the influence of temporally and spatially varying base states, in order to provide insight into the seasonal and regional variations that double-diffusive transport has been observed to undergo in the Dead Sea.

3.1. Double-diffusive salt fingering

As discussed in the preceding section, seasonal atmospheric temperature variations combine with the effects of evaporation to generate a stable thermohaline stratification of the water column during the summer months, characterized by a warmer and saltier epilimnion above

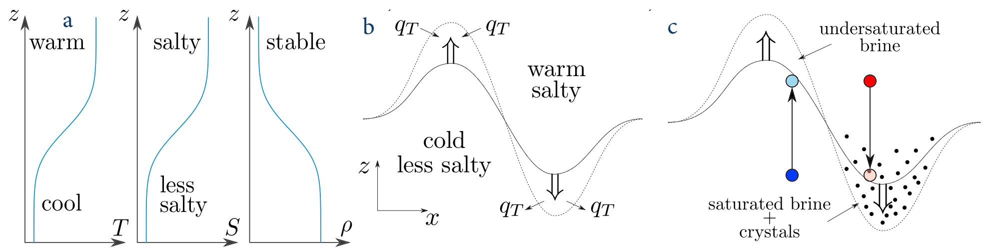

Figure 3

a) Temperature, salinity and density profiles in the Dead Sea during summer. b) Traditional double-diffusive salt fingering. c) Double-diffusive salt fingering under saturated conditions, with halite precipitation. The red (blue) fluid parcels initially in the epilimnion (hypolimnion) lose (gain) heat, while largely maintaining their salinity level (from Ouillon et al. 2019).

a colder, less saline hypolimnion, as shown in fig. 3a (Steinhorn, 1985; Anati et al., 1987; Arnon et al., 2016). This configuration renders the Dead Sea susceptible to double-diffusive fingering, an instability that evolves in stably stratified environments where two scalars with different diffusivities contribute to the density in opposite ways (Stern, 1960; Turner, 1974; Radko 2013). In the Dead Sea, heat represents the stabilizing fast diffuser, while salinity is the destabilizing, slow diffuser. Linear stability theory indicates that the emergence of double-diffusive salt fingering depends on the stability ratio R_ρ, which denotes the ratio of the contributions to the vertical density difference due to temperature and salinity, respectively. The water column is unstable to double-diffusion when $1 < R_\rho < 1/\tau$, where $\tau \approx 0.01$ is the ratio of the diffusivities of salt and heat in water. This double-diffusive instability triggers the formation of descending salt fingers that carry the warmer and saltier fluid parcels from the epilimnion into the colder and less salty hypolimnion, as shown in fig. 3b. Simultaneously, ascending fingers transport cooler, less salty hypolimnetic fluid upward into the epilimnion. The resulting net effect is a strong downward flux of dissolved salt from the epilimnion through the pycnocline (metalimnion) into the hypolimnion, accompanied by a weaker downward heat flux. Double-diffusive fingering has been studied in detail both theoretically (Stern, 1960; Stern and Turner, 1969; Huppert, 1971; Huppert and Turner, 1981), by means of laboratory experiments (Turner, 1967; Linden, 1971, 1973), via numerical simulations (Stern et al., 2001; Radko, 2003; Traxler et al., 2011), and through field observations (Hoare, 1966; Newman, 1976; Anati and Stiller, 1991; Wüest et al., 1992; Stevens and Lawrence, 1998; Sánchez and Roget, 2007; von Rohden et al., 2010; Arnon et al., 2016). An excellent review of the field is provided by Radko (2013).

3.2. Double-diffusive fingering in hypersaline water bodies: salt precipitation

As the only deep stratified hypersaline lake in the world that presently precipitates halite, the Dead Sea provides a unique natural laboratory for studying the coupling between salt fingering and saturation. During the 1979–1988 meromictic and holomictic periods, Anati and Stiller (1991) analyzed the Dead Sea with regard to its potential for triggering double-diffusive instabilities. Their measurements provided indirect evidence for the existence of double-diffusive fingering at $R_\rho = 1.7$, as they indicated a salinity decrease in the epilimnion commencing in August, with a concurrent salinity increase in the hypolimnion, which they could not explain without invoking double-diffusive fluxes. However, since the Dead Sea is periodically saturated with respect to halite, conclusive evidence that salt is

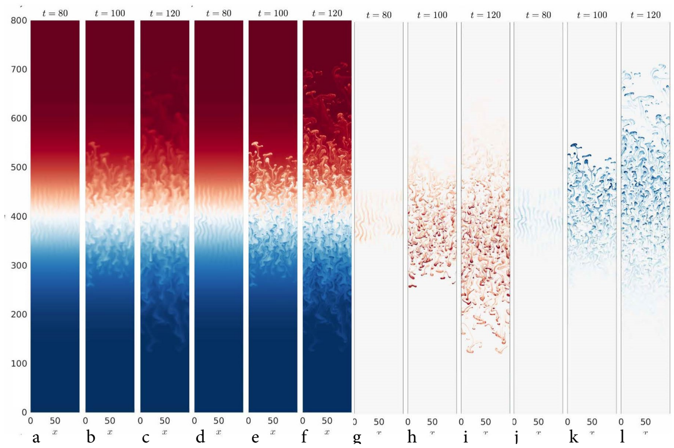

Figure 4

Double-diffusive salt fingering with precipitation; snapshots of the scalar fields at various times: (a-c) temperature, (d-f) brine salinity, (g-i) halite crystal concentration, (j-l) brine saturation. Red (blue) indicates higher (lower) values (from Ouillon et al. 2019a).

transported from the epi- to the hypolimnion by double-diffusive processes, as opposed to by the precipitation and settling of halite crystals, required additional observations that can differentiate between these processes. Such direct evidence for these processes was obtained more recently by Arnon et al. (2016), who were able to distinguish the roles of halite precipitation and double-diffusive salt fingering by in situ measurements that quantified the degree of halite saturation with very high accuracy (Sirota et al. 2016). As warm, salt-rich fingers descend from the surface layer into the hypolimnion and lose some of their heat, they can become supersaturated, so that halite crystals are expected to precipitate and sediment, cf. fig. 3c. Indeed, Arnon et al. (2016) were able to observe the formation of halite crystals just below the thermocline. They pointed out that, in contrast to traditional thermohaline fingering, salt fingers in saturated stratified brines are asymmetrical, in the sense that descending fingers cool and precipitate halite, whereas rising fingers gain heat, become undersaturated, and have the potential to dissolve halite. Sirota et al. (2017) studied the basin-scale implications of these processes for the formation of halite layers in deep hypersaline bodies of water, which will be further discussed in section 5.

3.3. Numerical simulations

Ouillon et al. (2019a) conducted highly resolved direct Navier-Stokes simulations which confirmed the hypothesis of Arnon et al. (2016) that double-diffusive salt fingering can account for the reduction of salinity in the epilimnion during midsummer, along with the precipitation of halite in the hypolimnion. The set-up for their simulations was guided by in-situ observations from the Dead Sea, in terms of temperature, salinity, saturation and halite crystallization rate, but focused on a laboratory-scale model water column. The authors assumed thermodynamic equilibrium, so that the maximum salinity of the brine is given by the solubility limit. Once the brine concentration reaches the solubility limit, any additional salt results in the formation of halite crystals. The difference between the salinity and the solubility limit is referred to as the saturation Sa.

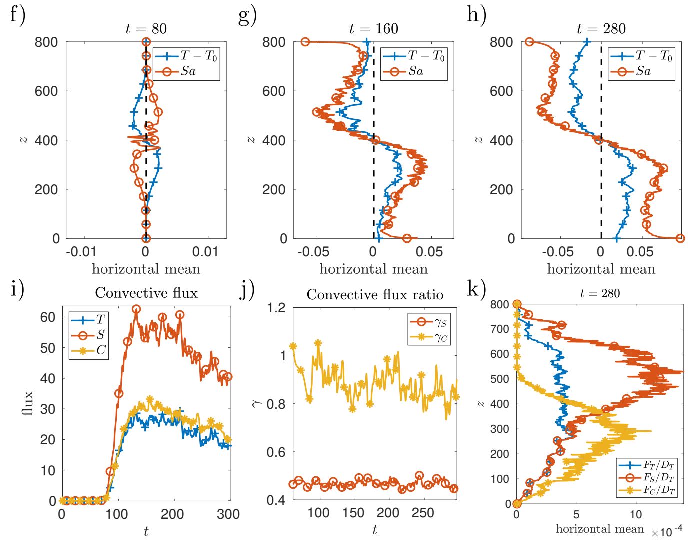

Figure 5

(f-h) Vertical profiles of horizontally averaged temperature change $T - T_0$ relative to initial conditions, and of the total saturation Sa, at three different times. The vertical black dashed line indicates zero, to facilitate the interpretation of the profiles. Note that the x-axes are scaled differently for better visibility. (i) Mean vertical convective fluxes of temperature T, dissolved salt S, and crystals C as functions of time. (j) Mean flux ratios as a function of time. (k) Horizontally averaged vertical flux profiles of temperature, dissolved salt, and halite (from Ouillon et al. (2019a).

Figure 4 shows a set of representative simulation results, in terms of temperature, solute salinity, halite crystal concentration and brine saturation. The figure indicates a double-diffusive convection regime at the center of the domain, with fingers propagating symmetrically up- and downwards away from the center. While the downward propagating fingers carry saltier and warmer fluid than the surroundings, those propagating upwards carry fresher, colder fluid. Above the pycnocline, salinity gradients are significantly steeper than temperature gradients (fig. 4a-f), due to the higher thermal diffusivity. Below the pycnocline, on the other hand, the brine is saturated and temperature and salinity gradients are of similar magnitude. This is a consequence of the temperature dependence of the solubility limit, which causes gradients of dissolved salinity to scale with the temperature gradients. Fig. 4g-i indicates that crystals are mostly found in the lower half of the domain, while fig. 4j-l indicates that the epilimnion tends to be undersaturated.

The vertical propagation of the double diffusion-driven halite precipitation can be observed in fig. 5. Frames f-h show horizontally averaged profiles of the difference between the instantaneous temperature T and the initial temperature T_0, and of the total saturation Sa, for three different times. During the early, diffusive stage (fig. 5f), before fingers form, the differential diffusion leads to a net transport of heat downwards, while salinity remains comparatively unchanged, thus generating supersaturated conditions right above the pycnocline and undersaturated conditions right below. As fingers form, however, the net downward transport of salt by the fingers increases the overall salinity in the lower half of the domain, and decreases it in the upper half. It is instructive to define the vertical fluxes of heat, dissolved salt and salt crystals, averaged over the entire computational domain. Fig. 5i

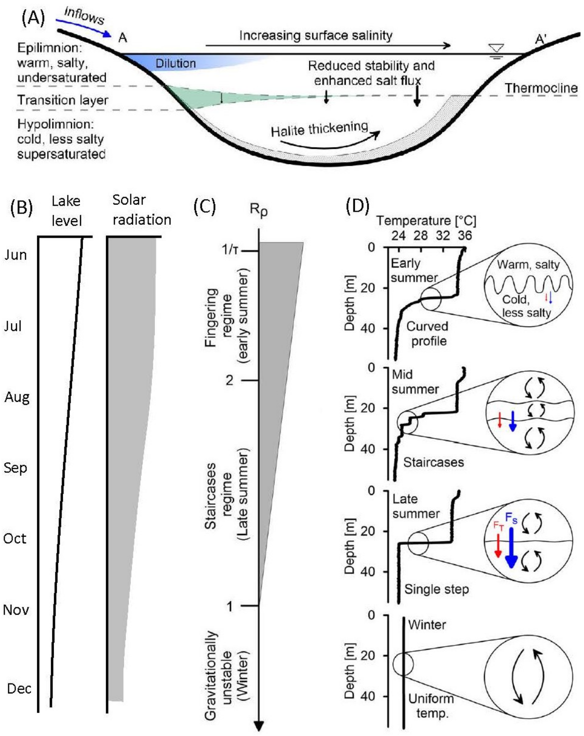

Figure 6

Regional and seasonal changes in the thermohaline stratification and the associated salt fingering: a) surface salinity increases from the northern end of the Dead Sea (left), where the Jordan river enters, towards its southern end (right); b) evaporation causes the lake level to decline throughout the summer, and surface salinity to increase; c) as surface salinity increases, the stability ratio R_ρ decreases throughout the summer, which promotes the formation of thermohaline staircases that enhance the downward salinity flux. During winter, the stability ratio drops below one, resulting in the entire water column to turn over and mix (modified after Sirota et al. 2020).

indicates that the salinity flux is roughly twice as strong as that of heat, consistent with the profiles shown in frames g and h. Interestingly the flux ratios γ_S (heat flux to dissolved salt flux) and γ_C (heat flux to salt crystal flux), calculated beyond the onset of instability, remain approximately constant in time, as shown in frame j. The horizontally-averaged vertical profiles of the vertical convective fluxes (fig. 5k) show how the metalimnion converts the epilimnion's downward dissolved salt flux into a downward halite crystal flux in the hypolimnion. In summary, the simulations confirm that double-diffusive salt fingering originating in the metalimnion results in the formation of antisymmetric total saturation profiles, with undersaturated brine in the upper layer and a mixture of saturated brine and halite crystals in the lower one.

3.4. Seasonal and regional variations in thermohaline stratification and halite deposition

The above laboratory-scale simulations and observations indicating that halite precipitates in the hypolimnion and is being dissolved in the epiliminion, focused on one-dimensional base states that depend on the vertical direction only. Nevertheless, they provide insight that can guide our expectations for base states involving temporal and spatial variations of salinity and temperature. Hence they can serve as a basis for interpreting the field observations by Mor et al. (2018) and Sirota et al. (2020), who investigate the influence of seasonal and regional hydroclimatic gradients over the lake surface in order to identify the origins behind spatial variations in the architecture of salt giants in deep hypersaline basins. These seasonal and regional variations are caused by the freshwater inflow from the Jordan river and several springs and smaller seasonal streams near the northern end of the Dead Sea, whereas the southern end is dominated by evaporation, cf. fig. 6a. Evaporation during the summer results in a lake level decline of $\sim 0.1m$ per month. This raises the surface salinity, so that the salinity difference between the epilimnion and hypolimnion increases from $\sim 0.4kg/m^3$ in April to $\sim 3kg/m^3$ in late July. During the same time interval, the temperature difference between the epilimnion and hypolimnion grows to $\sim 11°C$, so that the overall density stratification remains stable, but the stability ratio R_ρ decreases (fig. 6c). The field data of Sirota et al. (2020) and Arnon et al. (2016) indicate that the transition zone between the warm and salty upper layer and the cooler, less salty lower one begins to exhibit a thermohaline staircase as the summer progresses, i.e., a sequence of steep steps over which the temperature and salinity of the layers decrease. These steps merge in late summer, cf. fig. 6c, so that a single sharp step evolves, with a transitional layer less than $1m$ thick and a vertical temperature gradient of $9°C/m$. At the same time, the downward salt flux sharply increases to values in excess of $1kg/m^2$ per day during late summer, which is twice the effective surface salt flux due to evaporation. Qualitatively similar thermohaline staircasing has been observed in the ocean by Radko (2003), Schmitt (1981), Zodiatis & Gasparini (1996) and others, for stability ratios $R_\rho < 2$. Theory (Radko, 2003, 2013) and numerical simulations (Stellmach et al., 2011; Traxler et al., 2011) link this staircase formation to the growth of a secondary mean-field instability, the so-called γ-instability, which results in dramatically increased turbulent heat and salt fluxes. Sirota et al. (2020) analyzed the Dead Sea field observations of thermohaline staircases from the perspective of this γ-instability. Consistent with the theoretical predictions, they find that the onset of thermohaline staircases in mid-summer, as well as the associated increase in the salt flux, coincide with the drop of the stability ratio R_ρ below 2. As the authors point out, basic scaling considerations (Radko, 2013) indicate that the most unstable salt fingering mode in the Dead Sea has a horizontal wavelength of $O(5cm)$. Direct numerical simulations by Stellmach et al. (2011) demonstrate that the vertical wavelength of the first emerging horizontal layers, for conditions typical of the Dead Sea, is about one order of magnitude larger than this horizontal wavelength of the dominant salt fingering mode, so that we expect the first thermohaline staircases to appear with a thickness of $O(50cm)$, which again is consistent with the field observations.

The spatial variations in the thermohaline stratification mirror its seasonal evolution (Sirota et al. 2020). The freshwater inflows lower the surface salinity in the northern part of the lake, so that the surface salinity, and with it the salinity difference between epi- and hypolimnion, increase from north to south. Since the corresponding temperature difference is approximately uniform across the entire Dead Sea, the stability ratio R_ρ decreases from approximately 2.4 in the north to about 1.5 in the south, so that the northern temperature and salinity profiles remain smooth, while their southern counterparts are characterized by thermohaline staircases. As a result of this southward thermocline sharpening, the maximum vertical temperature gradient increases from 1 to $9°C/m$. The accompanying halite crystallization rate below the thermocline doubles from $0.2mm$ per day in the northern part to $0.4mm$ per day in the south. We note that halite crystallization is never observed above the thermocline during summers, as the downward heat and salt flux leave the epilimnion undersaturated.

In summary, the following picture emerges with regard to how regional and seasonal variations of the hydroclimate influence the growth of halite deposits on the lake floor: The salinity difference between epilimnion and hypolimnion increases until it peaks in late summer, and it is largest towards the south. The corresponding temperature difference grows during the build-up of the summer stratification, followed by late summer cooling, with little regional variation. Consequently, the stability ratio decreases monotonically throughout the summer and towards the drier south, which leads to the seasonal and regional sharpening of the thermocline, and the transition to thermohaline staircases and eventually to a single sharp step. This results in a larger downward salt flux in the south, which explains the increasing rates of halite crystallization observed near the southern end of the Dead Sea.

In the following, we will discuss how the metalimnion is being affected by internal waves along the pycnocline, and how the double-diffusive salt fluxes across the metalimnion affect the salt deposits on the lake floor.

4. INTERNAL AND SURFACE WAVES

Wind shear generates both waves and currents at the lake surface, which in turn can result in the emergence of standing waves known as seiches, and of internal waves that form and propagate along the pycocline (Bouffard and Boegman 2012). Such internal waves are known to grow to amplitudes of $O(1-10m)$ in lakes, depending on the density stratification of the water column, the external forcing, and the size and shape of the basin. A comprehensive review of our current knowledge on internal waves is provided by Sutherland (2010). As discussed in section 2, in the Dead Sea the density contrast between the epi- and hypolimnion varies seasonally, so that we expect corresponding seasonal variations for the internal wave dynamics (Arnon et al. 2016). The first systematic measurements of surface and internal waves in the Dead Sea were performed during five days in the summer of 1981 (Sirkes et al. 1997), followed by observations in 1994 (Weinstein et al. 2000) during the unusual three year meromictic period mentioned earlier (Stiller et al. 1984; Anati 1997; Gertman and Hecht 2002).

Arnon et al. (2019) conducted highly resolved measurements of both internal and surface waves during the stratified period from spring until autumn of 2012, employing fiber optic temperature profilers that measured vertical profiles with a resolution of $0.1m$ every 5 minutes, continuously for 7 months (Arnon et al. 2014). Fig. 7 presents their observational data for surface and internal wave heights, along with the wind speed, for two 10-day periods with different density contrasts across the pycnocline. The wind, as the primary driver of surface and hence internal waves, displays the typical $24hr$ period mentioned earlier. While the surface waves exhibit a characteristic amplitude of $O(1cm)$, the internal wave oscillations extend over a few meters, as expected from ratio the respective density differences across the pycnocline and the lake surface. Based on the layer heights and the density difference across the pycnocline, the phase velocity of the internal waves is estimated to be about $0.56m/s$ in August, and $0.37m/s$ in October, which is close to the measured values of $0.48m/s$ and $0.43m/s$ (Sutherland 2010, Arnon et al. 2019). For the

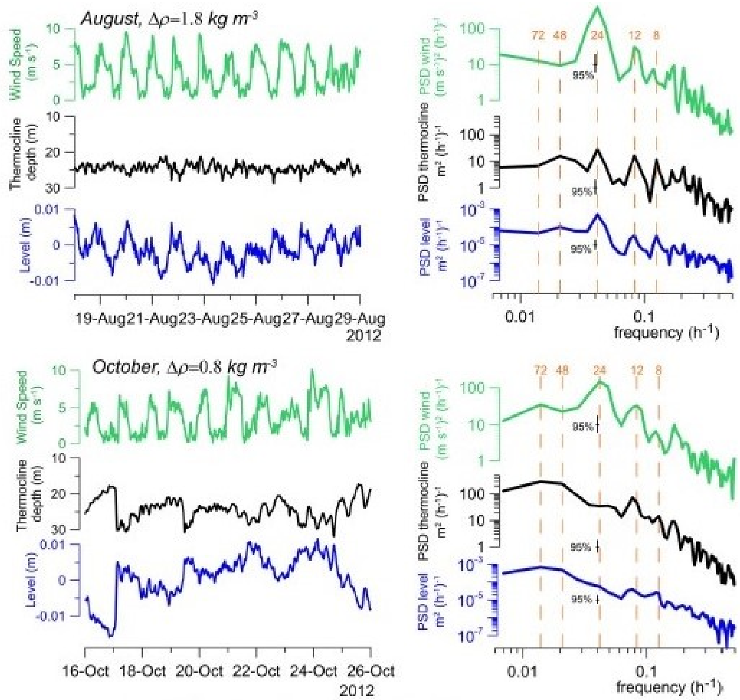

Figure 7

Time series and power spectra of wind speed (green), thermocline depth (black), and lake level (blue). Top: August 2012, bottom: October 2012. The vertical dashed orange lines indicate the corresponding time periods (from Arnon et al. 2019)

seiche mode, with a wavelength of twice the length of the Dead Sea, we obtain periods of $46.7h$ in August and $70.6h$ in October. Indeed, the internal wave spectra of fig. 7 indicate a significant amount of energy at these values.

The ongoing diversion of Jordan river inflows, and the reduced density contrast caused by it (see section 2), have resulted in much higher internal wave amplitudes over the last several decades. During the brief meromictic period from 1992 to 1995, the amplitude and period of the first internal mode were estimated to be approximately $3m$ and $20h$, respectively (Weinstein et al. 2000). This is in contrast to today's much larger internal wave amplitudes of $O(10m)$ and longer periods of 50 to $70h$.

4.1. Effect of Earth's rotation

For large lakes, the interplay of stratification, Earth's rotation and basin geometry can result in the formation of propagating cyclonic basin-scale internal waves, with typical periods ranging from hours to days (Bouffard and Boegman 2012). Earth's rotation, and with it the Coriolis force, becomes important when the Burger number $Bu = R_0/R < 1$, where R indicates the length scale of the basin, typically the lake radius, and $R_0 = C/f$ denotes the Rossby radius. Here C represents the wave velocity and $f = 4\pi\, sin\theta/T$ is the Coriolis parameter, with T denoting Earth's rotation period and θ the latitude. For the Dead Sea, we have $R \approx 15km$ and a typical October first-mode internal wave phase speed

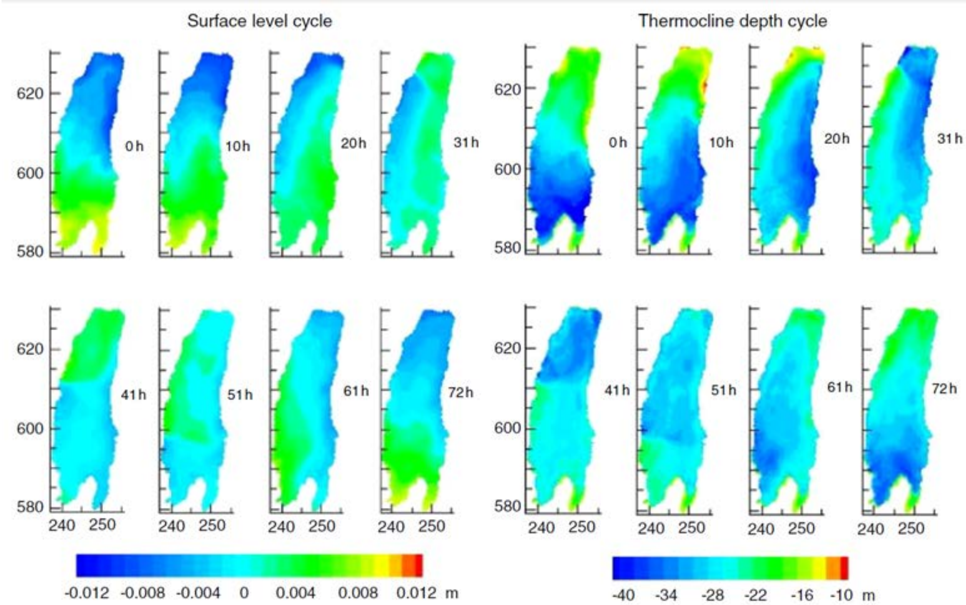

Figure 8

Simulated spatial progression of surface (left) and internal waves (right) for the three-day period from October 16, 2012, $00:00h$, to October 19, 2012, $00:00h$ (from Arnon et al. 2019).

$C = 0.37m/s$, which gives $R_0 \approx 5km$ and $Bu \approx 0.33$, which leads us to expect Earth's rotation to be influential. In order to check for the existence of cyclonic waves, Arnon et al. (2019) employed a computational model of the Dead Sea to perform three-dimensional simulations of the surface and internal wave dynamics. Consistent with the above scaling arguments, they observed cyclonic waves (counterclockwise in the northern hemisphere) with the surface and thermocline deformation being out of phase, as shown in figure 8.

5. EVOLUTION OF SALT DEPOSITS

In salt ponds and shallow natural hypersaline lakes (Lowenstein and Hardie 1985, Bowen et al. 2017) the precipitation and deposition of salt is usually limited to the dry season, when evaporative losses exceed inflows. Eventually, this imbalance causes the salinity level to reach the solubility limit, so that precipitation commences. The large deposits in Earth's crust known as 'salt giants,' on the other hand, with thicknesses of up to $O(1km)$, were deposited in deep hypersaline water bodies (Schmalz 1969, Hsu 1972, Hardie and Lowenstein 2004, Warren 2010, Sirota et al. 2020). As the only modern deep hypersaline lake on Earth, the Dead Sea is key to understanding the properties of these salt giants, including the processes governing their inception, growth, and geometrical features, as it allows for their direct observation.

Halite deposition in the Dead Sea was first observed in the early 1980s (Steinhorn 1983), concurrently with the transition from meromictic (no overturning) to holomictic (annual overturning) conditions. An order-of-magnitude estimate of the depositional rate on the lake floor can be obtained from a global mass balance argument: for each meter that the level of a saturated water column drops, an increase in the deposit thickness of

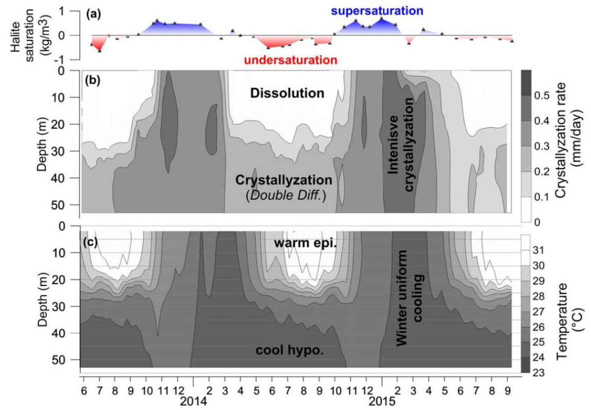

Figure 9

a) Time series of halite saturation in the epilimnion at $10m$ depth; b) and c) depth-time diagram of halite precipitation rates (cable measurements) and temperature, respectively. During summer, with evaporation reaching its peak, the warmer epilmnion is nevertheless under-saturated and dissolves halite, due to the temperature dependence of solubility. However, double-diffusive salt fingering maintains a constant inflow of salinity into the lower hypolimnion, so that it keeps depositing halite even during summer. Saturation is highest and precipitation is strongest during the winter months.

about $10cm$ is expected (Lensky et al. 2005, Sirota et al. 2021). However, this simple estimate can provide only a partial explanation of what has been observed over the last 45 years. New limnological and sedimentological measurements conducted in the Dead Sea over the last decade (Arnon et al. 2016, Sirota et al., 2016, 2017, 2020, 2021) have fundamentally reshaped our understanding of the processes governing the growth of deep-water salt deposits. In particular, these authors observed that halite deposition is most intense during the winter months, when the entire well-mixed water column cools so that its solubility level is reduced. During this season, halite precipitation occurs throughout the entire water column, cf. fig. 9. In contrast, during summer the epilimnion above the thermocline warms significantly, which renders it undersaturated. Consequently, this upper layer can partially or even completely dissolve halite that was previously deposited on the lake floor, down to the level of the thermocline at approximately $25m$. At the same time, the double-diffusive salt flux from the epilimnion downward through the thermocline, discussed in section 3, provides a continuous source of salt for the cooler hypolimnion in the deeper sections of the Dead Sea even during the summer months, so that this part of the lake remains supersaturated and continues to precipitate halite even during summer (fig. 9). The net result is a 'halite focusing' effect that transports salt from the shallow lake floor above the thermocline towards the deep lake floor below the thermocline (Sirota et al. 2017, 2018), cf. fig. 10. This thickening towards the deep sections of the lake has also been observed for salt giants in the geological record, such as the Mediterranean salt deposits described by Kirkham et al. (2020).

Several key differences have been observed regarding the nature of the halite deposits that form during different times of the year (Sirota et al. 2017). During the winter, when the entire water column is highly supersaturated, small cubic crystals of $O(0.1mm)$ diameter precipitate throughout the entire water column and settle on the lake floor, forming a smooth and uniform deposit (fig. 1c). During the summer, on the other hand, when the

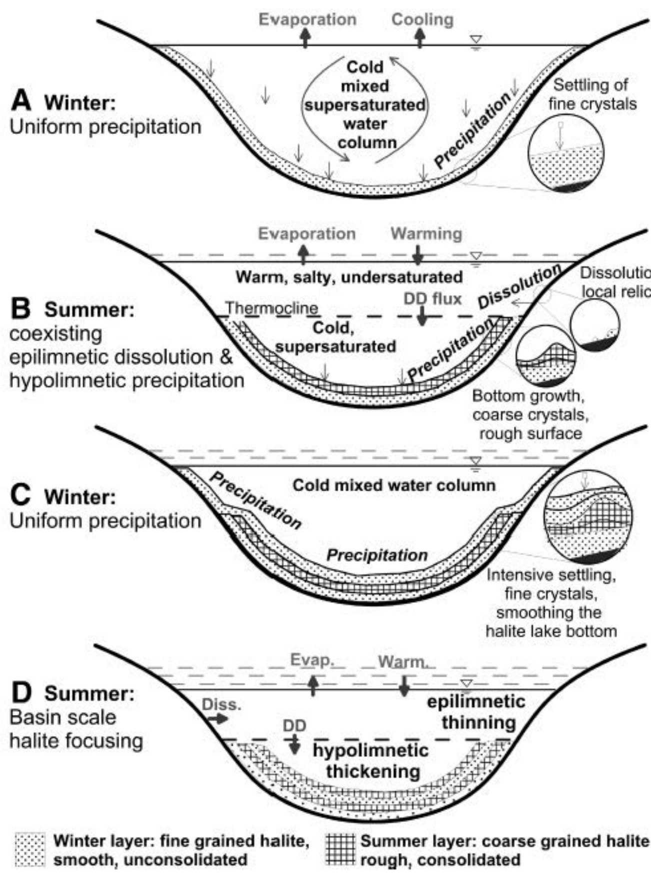

Figure 10

During summers, the shallow epilimnion is undersaturated and dissolves halite deposits, while coarse crystals and a rough deposit surface form along the deep lake floor. During winter, fine crystals precipitate throughout the entire water column and yield a smooth surface of the halite deposit. This seasonal pattern results in a shallow lake floor with minimal halite deposits, and a deep lake floor with alternating layers of fine and coarse halite deposits (after Sirota et al. 2017)

hypolimnetic layer near the lake floor is only slightly supersaturated, coarse cubic halite crystals of $O(5mm)$ form on the lake floor (fig. 1e) and yield a rough deposit surface, since low supersaturation favors the growth of existing crystals over the formation of new nuclei. These rough deposits can form 'domes' that are tens of centimeters wide and high (fig. 1d). Sirota et al. (2017) proposed that these domes develop as a result of a positive feedback mechanism regading the salinity flux across the concentration boundary layer near the lake floor. Above deposit peaks the salinity boundary layer is thinner, so that its gradient is steeper than above the valleys. Hence the salinity flux to the peaks is larger than to the valleys, and the peaks keep growing more rapidly. However, quantitative details of these processes are not understood at present.

The 'salt chimneys' shown in fig. 1f tend to grow at the locations of springs on the Dead Sea floor. The discharged spring water is less dense than the ambient Dead Sea brine and forms a buoyant plume. Due to the different chemical compositions of the spring water and the ambient brine, calcium carbonate (aragonite) and calcium sulfate (gypsum) precipitate where they mix. As the hollow chimney grows, the source of the spring migrates upwards and halite also deposits on its outside.

6. BEACH FEVOLUTION UNDER RAPID SEA LEVEL DECLINE

During the winter months, storm waves transport and sort both fine sediment and coarse gravel along so-called 'coastal conveyors' near the shoreline (Celikoğlu et al.; 2004, Masselink et al., 2014), leading to the formation of sandbars, beach berms and other features that display characteristic length scales and sorting properties. With the end of the stormy winter season, these properties are being preserved, as the rapid sea level decline of about $1m$ during the subsequent summer months leads to their 'fossilization' on the newly formed beaches, where they are easily accessible. Hence they can be investigated in detail, in order to obtain insight into the evolution of coastlines and beaches under changing sea levels and increased storm frequency and intensity. This information is essential for the further development of models for coastal gravel sorting that can inform coastal management of longshore transport (McLaren and Bowles, 1985; Masselink, 1992; Brand et al., 2020).

Eyal et al. (2021) investigated how coastal gravels get sorted in the Dead Sea, i.e., their alongshore displacement and ordering according to mass by storm waves. The storms are related to synoptic-scale Mediterranean cyclones (Arnon et al., 2019; Dayan and Morin, 2006), which generate 10–15 southwestern to southern windstorms per winter, each lasting from a few hours to three days, and blowing over approximately $40km$ of lake fetch. Consequently, the distribution of wave heights is narrow and largely unaffected by dispersion. Waves propagate from south to north and approach the coast at approximately 45°, so that they form optimum conditions for unidirectional longshore drift (Longuet-Higgins, 1970; Van Hijum and Pilarczyk, 1982). The steady component of the longshore currents, driven by either winds or wave radiation stresses (Bowen, 1969; Longuet-Higgins, 1970) is about an order of magnitude less than the wave orbital velocity, so that the coarse gravel transport is dominated by the waves. The investigation by Eyal et al. (2021) focused on a specific field location where coarse gravel is supplied to the coast of the Dead Sea by a seasonal stream that is connected to the receding coastline by cross-shelf incision (Eyal et al. 2019). The unsorted gravel is delivered by flash floods and subsequently transported underwater by storm waves, alongshore in the northward direction. The authors observe the formation of well-sorted beach berms, along which the gravel size decreases with distance. As a result of lake level decline, each gravel berm is associated with a specific winter season by that season's lake level (fig. 1b). The gravel transport occurs under strong winds with speeds up to $20m/s$, which generate waves with a maximum height of about $4m$, typical periods of $4s$, and characteristic wavelengths of $25m$. The authors furthermore employ 'smart boulders' equipped with accelerometers that record their real-time motion and allow for the measurement of longshore displacement during individual storms (fig. 11).

Eyal et al. (2021) couple their field observations of intra-storm gravel transport and sorting with the development of corresponding scaling laws, based on the wave characteristics and the associated hydrodynamic pressure force and impulse exerted on the gravel. By employing linear wave theory, they arrive at the prediction that the critical wave height for incipient motion H_{cr} scales as $H_{cr} \sim M^{1/6}$, where M represents the mass of the submerged gravel. This scaling relationship agrees well with their field observations (fig. 11g).

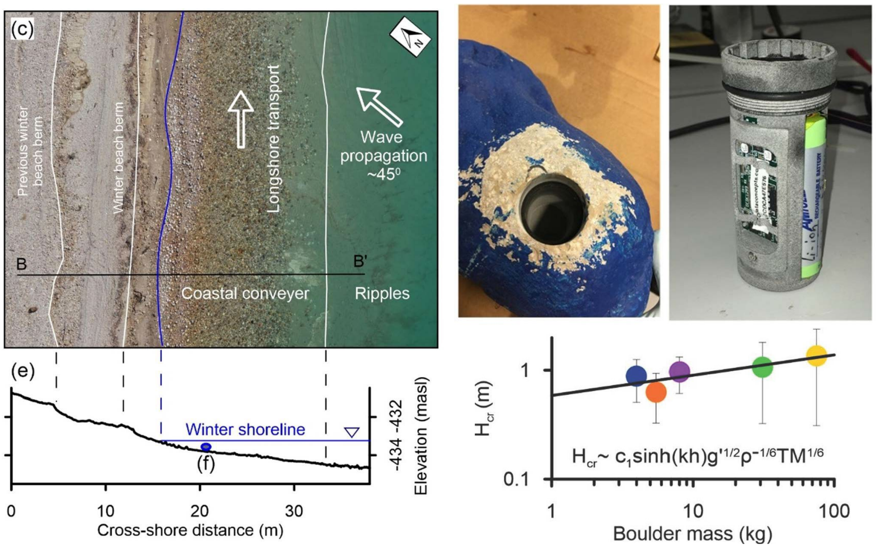

Figure 11

c) Aerial photograph of the active conveyor, and the directions of longshore transport and wave propagation during storms; e) Topographic profile across the active coastal conveyor; f) Smart boulder and logger; g) Critical wave height H_{cr} for boulder mobilization, as a function of boulder mass M. Measured values using smart boulders are indicated by color dots. The black line with the predicted exponent 1/6 yields good agreement with the measured values (after Eyal et al. 2021).

Once a boulder is in motion, its average displacement δ within a single period of a wave with height H can be obtained by considering the net impulse exerted on the gravel, which yields $\delta \sim M^{1/3}(H^2 - H_{cr}^2)$. The overall displacement of a gravel during a storm then depends on the wave spectrum and the duration of that particular storm. Eyal et al. (2021) demonstrate that the above scaling arguments align with corresponding field observations.

7. INCISION OF SEASONAL RIVERS UNDER LAKE LEVEL DECLINE

In response to the lake level decline over the past several decades, the streams draining into the Dead Sea have been cutting through the newly exposed erodible sediment bed filling the basin (figs. 1h, 12). As the coastline recedes, the stream mouth cuts into the newly formed beach and steepens the local slope of the stream bed. This region of enhanced incision then migrates upstream, thereby resulting in a transient response along the entire length of the stream bed. Highly resolved digital elevation data have enabled the careful analysis of this process for both ephemeral tributaries that flow during flash floods (Ben Moshe et al. 2008, Bowman et al. 2010, Eyal et al., 2019), as well as for perennial streams including the Jordan river (Hassan and Klein 2002, Vachtman and Laronne 2013, Dente et al. 2017, 2018, 2021). Following earlier work of Begin (1978) and Begin et al. (1981), and by employing several simplifying assumptions, Ben Moshe et al. (2008) were able to develop a numerical sediment flux model that reproduces this dynamic evolution. Such models can be valuable for planning purposes in environments with rapid sea level decline, where incision may pose a risk to infrastructure.

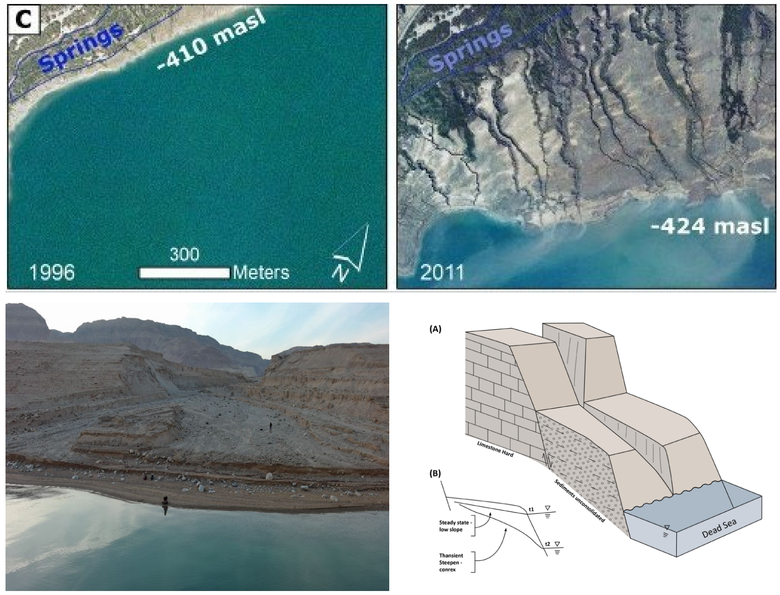

Figure 12

a,b) Aerial photos of newly exposed beach show the formation of deeply incised channels between 1996 and 2011 (Dente et al. 2021); c) Upstream view of Nahal Darga from the stream mouth, note the person at the water's edge for scale (photo courtesy of Liran Ben Moshe); d) Conceptual sketch of stream bed incision and upstream migration of the knickpoint in response to the lake level fall. The exposure of steep slope at the stream mouth leads to the steepening of the stream bed, which acquires a convex curvature.

Eyal et al. (2019) focused on the present Dead Sea to investigate the transport of coarse sediments in streams during sea level decline, a common scenario for lakes and reservoirs in arid regions of the world, as well as along receding continental coastlines during interglacial periods (e.g., Woolfe et al. 1998, Törnqvist et al. 2006). The authors showed that as a low-gradient continental shelf emerges, initially alluvial fans form. Upon the subsequent exposition of the continental slope, the upstream-propagating incision of the stream bed then starts a positive feedback loop where the channel narrows, so that water height, shear stress and sediment flux in the stream bed increase. Consequently, coarse sediments can be transported across the entire exposed shelf to the lowstand shoreline. Eyal et al., (2019) furthermore explored spatio-temporal variations in the mobility and transport of sediments as a function of when and where the local bed stress exceeds a critical Shields stress value (Shields 1936, Buffington and Montgomery 1998). The authors demonstrated that if this critical value is exceeded everywhere along the stream, sediment can effectively bypass the entire shelf.

Interestingly, the perennial streams draining into the Dead Sea exhibit a tendency for increased meandering along sections where the channel slope steepens (Dente et al., 2017, 2018). This finding is somewhat unexpected, as rivers typically meander across flat plains rather than on steep slopes. On the other hand, experiments by Schumm and Khan (1972) had shown that meandering as an instability phenomenon intensifies for steeper channel slopes. The recent lake level decline of the Dead Sea enabled Dente et al. (2021) to study this phenomenon for a rare, field-scale set of a dozen adjacent perennial channels

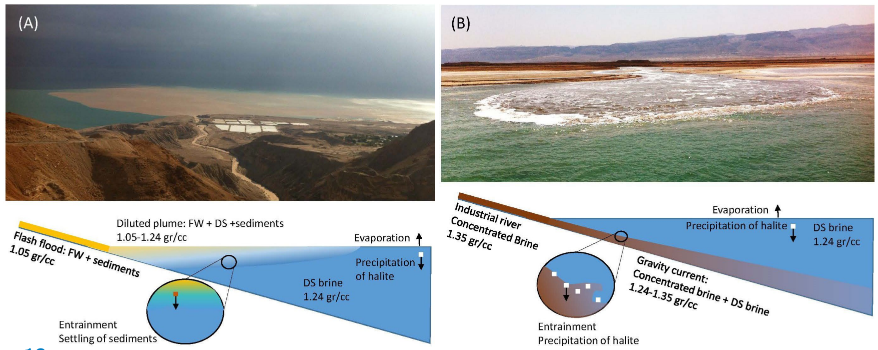

Figure 13

a) Positively buoyant river plume formed by an ephemeral stream discharging a flash flood; b) Negatively buoyant river plume of the industrial Nahal Ha'Arava stream that carries dense brines generated by the local potassium industry into the southern Dead Sea.

evolving in a homogeneous erodible substrate. These channels were initially straight and subsequently transformed into incising, meandering channels as preexisting, steeper lake bathymetry emerged. The authors furthermore observed the highest sinuosity along the steepest channel sections, which also developed the deepest and widest valleys.

8. OPEN QUESTIONS

The inflow of perennial streams such as the Jordan river, and of ephemeral streams that discharge flash floods, gives rise to a host of complex phenomena that are poorly understood at present. At the stream mouths, positively buoyant sediment-laden freshwater plumes form and spread laterally as surface gravity currents, driven primarily by the large density difference with respect to the ambient halite-saturated brine (fig. 13a). This density difference is much larger than for typical ocean plumes and can reach values in excess of 20%. Quantifying the plume dynamics along with the associated sedimentation processes requires insight into the following mechanisms and their coupling: (i) the mixing and entrainment behavior across the large density gradient at the base of the plume; (ii) the lateral spreading of the particle-laden surface plume as a buoyant gravity current; (iii) the heat, mass and momentum exchange at the air-water interface under the influence of evaporation and wind, including their dependence on the concentration of dissolved salts; (iv) the settling of the suspended particles from the plume, possibly involving double-diffusive sedimentation (Burns and Meiburg 2012, 2015); (v) precipitation and settling of salt in response to surface evaporation and cooling (Ezraty et al. 2023); and (vi) convection driven by surface evaporation and cooling, along with the associated salinity increase. Progress on these issues and their dependence on the stratification of the water column will require field observations (e.g., Mor et al. 2018, 2021, Sirota et al. 2021) along with the development of simplified transport models for heat, mass and momentum, as well as numerical simulations. Predictive models of these processes will be essential in light of such proposed projects as the Red Sea-Dead Sea canal, which would result in the formation of a large plume in the Dead Sea that will exhibit novel biogeochemical processes (Gavrieli et al. 2011). Additional geological implications include the composition and distribution of both detritic and salt deposits in the vicinity of the plumes.

An unusual situation is presented by the perennial Nahal Ha'Arava stream that discharges into the southern part of the Dead Sea and carries very dense brines ($1.35 g/cm^3$) rejected by the local potassium industry, *viz.* the Israeli Dead Sea Works and the Arab Potash Company (Dente et al. 2017). These brines originate in evaporation ponds that raise the potassium concentration until potassium-bearing salt (Carnallite) precipitates. After the Carnallite is harvested, the remaining brine is discharged into the Dead Sea via the Nahal Ha'Arava river. Upon reaching the Dead Sea, this dense brine propagates along the lake floor of the Dead Sea as a hyperpycnal gravity current (fig. 13b, Lensky et al. 2011a,b, 2013, Kostachuk et al. 2018, Ouillon et al. 2019b, Schuch et al. 2021). As the Dead Sea brine and the potassium brine mix, halite precipitates out so that a salt delta develops near the stream mouth (Lensky et al. 2010c). During the summer, when the ambient water column in the Dead Sea is stratified, the hyperpycnal gravity current will initially advance through the less dense epilimnion, then cross the pycnocline, and subsequently propagate along the lake floor through the denser hypolimnion. Especially the interaction of the dense bottom current with the stratified density field of the pycnocline can give rise to a range of interesting phenomena such as the generation of internal waves and the 'decapitation' of the gravity current, as was previously observed in laboratory experiments and numerical simulations (Ouillon et al. 2019b). Very little is currently known about the nature of such phenomena in the Dead Sea.

Compared to freshwater lakes and the oceans, the significantly higher density and viscosity of the Dead Sea (Weisbrod et al. 2016) greatly increase its capacity to erode and transport sediments. As discussed in section 6, investigations have been conducted into the longshore sorting and transport of coarse gravel from stream mouths (Eyal et al. 2021). However, a number of questions remain unresolved, and finding answers will require additional field investigations and laboratory experiments, accompanied by model development. Among them are the transport and sorting of finer sediment emanating from stream mouths and the associated plumes, especially under the action of turbulent surface and bottom currents, and of wave fronts with various incident angles (Nehorai et al., 2013). Similarly, the sedimentation of these fine particles to the lake floor involves a host of complex process such as double-diffusive and other instabilities, and potentially aggregation (Burns and Meiburg 2012, 2015, Vowinckel et al. 2019). Eventually these sediments form deposit layers on the lake floor, so-called detritic laminae, that alternate with layers of salt deposits. As these lake floor deposits accumulate over long periods of time, they build a sedimentary archive that holds information for reconstructing past environmental conditions (Sirota et al., 2017, 2021, 2023, Ben Dor et al., 2021). It is the interaction among all of the above processes that governs the source-to-sink processes shaping these sedimentary archives embedded in the geological record, including the salt deposits and the inter-bedded detritic laminae.

Finally, the possibility of having alternating periods of lake level decline and lake level rise over longer time scales poses interesting questions regarding the long-term evolution of the water column's stability and the associated halite deposits. During periods of lake level decline, such as it is currently occurring, the overall salinity increases and the stratification of the water column becomes less stable, resulting in annual overturns. During periods of lake level rise, on the other hand, the overall salinity is reduced and the water column becomes more stable. It is evident that this process can involve significant hysteresis, in the following sense: if the surface level of a saturated lake passes through an intermediate height while declining, it will remain saturated, and the lake will keep depositing halite. On the other hand, if the lake's surface passes through the same height while its level is increasing, it is continuously being diluted, so that its salinity level will remain below saturation and it will not deposit. Similarly, for the same surface level of a lake, coastal erosion processes can also be quite different, depending on whether the lake level is rising or falling, with higher coastal erosion during lake level rise (Enzel et al. 2022). It is important to account for such hysteresis phenomena when trying to understand natural climate cycles and the signatures they leave behind in the geological record, but also for assessing the environmental impacts of infrastructure projects such as the Red Sea-Dead Sea canal.

9. CONCLUSIONS AND OUTLOOK

This review highlights some of the unique environmental settings of the Dead Sea that give rise to flow phenomena, transport processes and deposit characteristics that cannot be observed anywhere else on Earth at the present time. Most prominent among these unique conditions are the Dead Sea's very high salinity, great depth and rapidly falling lake level, as well as the mutual interactions among these features.

The Dead Sea's nature as a terminal lake, in conjunction with its declining surface level, has led to a dramatic increase of its salinity over the last few decades, to the point where it precipitates large amounts of halite on the lake floor year-round. At the same time, its substantial depth allows for the formation of a thermo- and pycnocline during the summer, which results in strong seasonal variations of the processes governing the formation of halite. During summer, the stably stratified water column gives rise to pronounced double-diffusive fingering between the epi- and hypolimnion, and to the precipitation of halite from the supersaturated descending fingers. During winter, on the other other hand, the entire water column is well-mixed and supersaturated, so that halite particles form and settle at all depths. As discussed, the annual overturns of the water column represent a relatively recent phenomenon, one that could possibly be reversed if a large engineering project such as the proposed Red Sea-Dead Sea canal were to carry large amounts of less salty water into the Dead Sea, thereby raising its lake level.

The rapid lake level decline of $O(1m/yr)$ over the last several decades has exposed vast areas of newly formed beach every year, which preserves valuable information regarding the formation of beach berms, and the transport and sorting of gravel and finer sediment which enters the Dead Sea via ephemeral streams that discharge flash floods. These transient streams incise deeply into the newly exposed beach areas, which allows for real-time observations of their meandering behavior and knickpoint migration. All of these observations provide valuable lessons for coastlines around the world with the regard to their stability and erosion under sea level change.

Numerous interesting questions remain open, especially with regard to the processes and mechanisms that govern spatial variations in the thickness of the halite deposits, as well as seasonal changes in their surface roughness. While recent investigations into vertical and horizontal variations of the salinity level in the water column have provided some insight, further progress is needed to obtain a more comprehensive understanding of the enigmatic salt giants observed in the geological record.

SUMMARY POINTS

1. As the only deep hypersaline lake on Earth today that precipitates salt, the Dead Sea provides a unique opportunity to explore buoyancy-driven multiphase flows

coupled to precipitation and dissolution, and how these shape the 'salt giants' found in the geological record.
2. Double-diffusive salt fingering across the thermocline maintains the salinity of the lower layer at saturation even during the summer, when the upper layer is under-saturated, thus enabling the Dead Sea to precipitate salt year-round.
3. The lake level of the Dead Sea is falling at about $1m/yr$, which provides opportunities for investigating the stability, erosion and sediment transport associated with arid coastlines under sea level change, along with measures for their protection.
4. Further studies are necessary to assess the potential impacts of resource extraction operations, and of proposed major infrastructure projects.

FUTURE ISSUES

1. How do the strongly stratified surface plumes evolve that exist at the inflows of rivers and streams, and how do they affect the deposition of sediment and salt?
2. Which buoyancy-driven flows involving precipitation shape the geometrical features of the salt deposits, including 'salt chimneys' and 'domes'?
3. Which processes govern the formation and growth of salt deltas at the inflows of hypersaline industrial brines?
4. How will the freshly exposed beaches evolve that include both shelf-like regions and steep slopes, along with deeply incising streams?

DISCLOSURE STATEMENT

The authors are not aware of any affiliations, memberships, funding, or financial holdings that might be perceived as affecting the objectivity of this review.

ACKNOWLEDGMENTS

E.M. and N.G.L. thank the members of their research groups at UC Santa Barbara (UCSB) and at the Dead Sea Observatory of the Geological Survey of Israel (GSI) for their invaluable contributions, especially Bernhard Vowinckel, Raphael Ouillon, Ido Sirota, Ali Arnon, Haggai Eyal, Roie Ezraty and Ziv Mor, as well as Isaac Gertman, Vladimir Lyakhovsky, Yehouda Enzel and Liran Ben Moshe for their long term collaboration in the study of the Dead Sea. E.M. furthermore gratefully acknowledges the hospitality of Shmuel Rubinstein, the Hebrew University of Jerusalem, and the GSI, during an extended visit as a Lady Davis Visiting Professor. In turn, N.G.L appreciates the warm hospitality during his and his students' visits to UCSB. Funding for this work has been provided by the Lady Davis Fellowship Trust, the U.S. National Science Foundation (NSF-1936358), the Israel Science Foundation (#1471/18), the Binational Science Foundation (2019/637), the Army Research Office, and the Engineer Research and Development Center of the Army Corps of Engineers. Inevitably in an article of this type there are omissions. Some are a result of choices forced by space limitations; others are mere oversights. To those whose work is not adequately acknowledged, we offer our apologies.

LITERATURE CITED

Anati, D. A., M. Stiller, S. Shasha, and J. R. Gat. (1987) Changes in the thermohaline structure of the Dead Sea: 1979–1984. Earth Planet. Sci. Lett. 84: 109–121.

Anati, D. A. (1997), The hydrography of a hypersaline lake, in The Dead Sea: The Lake and its Setting, edited by T. M. Niemi, Z. Ben-Avraham, and J. R. Gat, pp. 89–103, Oxford Univ. Press, Oxford.

Anati, D. A., and M. Stiller. (1991). The post-1979 thermohaline structure of the Dead Sea and the role of double diffusive mixing. Limnol. Oceanogr. 36: 342–353.

Arnon, A., Lensky N.G., and Selker J.S. (2014) High-resolution temperature sensing in the Dead Sea using fiber optics. Water Resour. Res., 50

Arnon, A., Selker, J.S. and Lensky, N.G. (2016) Thermohaline stratification and double diffusion diapycnal fluxes in the hypersaline Dead Sea. Limnol. Oceanogr., 61, 1214–1231.

Arnon, A., Brenner S., Selker J.S., Gertman I., and Lensky N.G. (2019). Seasonal dynamics of internal waves governed by stratification stability and wind: Analysis of high resolution observations from the Dead Sea. Limnology and Oceanography, 64

Begin, Z.B., (1978). Aspects of Degradation of Alluvial Channels in Response to Base-level Lowering. Geological Survey of Israel Report GSI-8-1978. 239 pp.

Begin, Z.B., Meyer, D.F., Schumm, S.A., 1981. Development of longitudinal profiles of alluvial channels in response to base-level lowering. Earth Surf. Proc. Landf. 6, 49–68.

Ben Dor Y., Marra F., Armon M., Enzel Y., Brauer A., Schwab M.J., and Morin E. (2021) Hydroclimatic variability of opposing late Pleistocene climates in the Levant revealed by deep Dead Sea sediments. Climate of the Past 17(6), 2653-2677.

Ben-Moshe L, Haviv I, Enzel Y, Zilberman E, Matmon A. 2008. Incision of alluvial channels in response to a continuous base level fall: field characterization, modeling, and validation along the Dead Sea. Geomorphology 93: 524–536

Beyth, M., Gavrieli, I., Anati, D.A. and Katz, O. (1993) Effects of the December 1991 - May 1992 floods on the Dead Sea vertical structure. Isr. J. Earth Sci., 42, 45–47.

Bouffard and Boegman 2012, Encyclopedia of Lakes and Reservoirs, Springer.

Bowen, A. J. (1969). The generation of longshore currents on a plane beach. Journal of Marine Research, 27(2), 206–215.

Bowen, B.B., Kipnis, E.L. and Raming, L.W. (2017) Temporal dynamics of flooding, evaporation, and desiccation cycles and observations of salt crust area change at the Bonneville Salt Flats, Utah. Geomorphology, 299, 1–11.

Bowman, D., Svoray, T., Devora, S., Shapira, I., Laronne, J.B. (2010) Extreme rates of channel incision and shape evolution in response to a continuous, rapid base-level fall, the Dead Sea, Israel. Geomorphology, 114(3), 227-237.

Brand, E., Chen, M., and Montreuil, A.-L. (2020). Optimizing measurements of sediment transport in the intertidal zone. Earth-Science Reviews, 200, 103029.

Buffington, J.M., Montgomery, D.R. (1998). A systematic analysis of eight decades of incipient motion studies, with special reference to gravel-bedded rivers. Water Resources Research 33: 1993–2029.

Burns, P. and Meiburg, E. 2012 Sediment-laden Fresh Water above Salt Water: Linear Stability analysis, J. Fluid Mech. 691, 279

Burns, P. and Meiburg, E. 2015 Sediment-laden Fresh Water above Salt Water: Non-linear Simulations, J. Fluid Mech. 762, 156-195.

Celikoğlu, Y., Yuksel, Y., and Kabdaşlı, M. S. (2004). Longshore sorting on a beach under wave action. Ocean Engineering, 31(11–12), 1351–1375.

Dayan, U. and Morin, E. (2006). Flash flood – Producing rainstorms over the Dead Sea: A review. New Frontiers in Dead Sea paleoenvironmental research: Geological Society of America Special Paper, 401(04), 53–62.

Dente, E., Lensky, N. G., Morin, E., Grodek, T., Sheffer, N. A., Enzel, Y. (2017). Geomorphic response of a low-gradient channel to modern, progressive base-level lowering: Nahal Ha'Arava, the Dead Sea. J. Geophys. Res.: Earth Surface, 122(12), 2468–2487.

Dente, E., Lensky, N. G., Morin, E., Dunne, T., Enzel, Y. (2018). Sinuosity evolution along an incising channel: New insights from the Jordan River response to the Dead Sea level fall. Earth Surface Processes and Landforms, 44, 781–795.

Dente, E., Lensky, N.G., Morin, E., Enzel, Y. (2021) From Straight to Deeply Incised Meandering Channels: Slope Impact on Sinuosity of Confined Streams. Earth Surface Processes and Landforms.

Enzel, Y., Mushkin, A., Groisman, A., Calvo, R., Eyal, H., Lensky N.G. (2022) The modern wave-induced staircase morphology of the coastal cliffs along the western Dead Sea. Geomorphology, 408.

Eyal, H., Dente, E., Haviv, I., Enzel, Y., Dunne, T., Lensky, N. G. (2019). Fluvial incision and coarse gravel redistribution across the modern Dead Sea shelf as a result of base-level fall. Earth Surface Processes and Landforms, 44, 2170–2185.

Eyal, H., Enzel, Y., Meiburg, E., Vowinckel, B., Lensky, N. G. 2021 How does coastal gravel get sorted under stormy longshore transport? Geophys. Res. Lett., 48, e2021GL095082.

Eyal H., Armon, M., Enzel, Y., Lensky, N.G. (2023) Synoptic- to meso-scale circulation connects fluvial and coastal gravel conveyors and directional deposition of coastal landforms in the Dead Sea basin. Earth Surface Dynamics

Ezraty, R., Rubinstein, S., Lensky, N., Meiburg, E. (2023) Interacting density fronts in saturated brines cooled from above. Journal of Fluid Mechanics 975.

Gavrieli, I. (2011). Dead Sea Study. Jerusalem.

Genin, A., B. Lazar, and S. Brenner. (1995). Vertical mixing and coral death in the Red Sea following the eruption of mount Pinatubo. Nature 377: 507–510.

Gertman, I., and A. Hecht (2002), The Dead Sea hydrography from 1992 to 2000, J. Mar. Syst., 35(3–4), 169–181.

Gertman, I., Kress, N., Katsenelson, B., Zavialov, P. (2010). Equations of state for the Dead Sea and Aral Sea: Searching for common approaches. (April).

Halpert, M. S., C. F. Ropelweski, T. R. Karl, J. K. Angell, L. W. Stowe, R. R. Heim, A. J. Miller Jr., and D. R. Rodenhuis. (1993). 1992 brings return to moderate global temperatures. Eos Trans. Am. Geophys. Union 74: 433–439.

Hardie, L. A., and Lowenstein, T. K. (2004). Did the Mediterranean Sea dry out during the Miocene? A reassessment of the evaporite evidence from DSDP legs 13 and 42A cores. Journal of Sedimentary Research, 74(4), 453–461.

Hassan MA and Klein M. (2002). Fluvial adjustment of the Lower Jordan River to a drop in the Dead Sea level. Geomorphology 45: 21–33.

Hoare, R. A. (1966). Problems of heat transfer in Lake Vanda, a density stratified Antarctic Lake. Nature, 210(5038), 787–789.

Hsu, K. J. (1972). Origin of saline giants: A critical review after the discovery of the Mediterranean evaporite. Earth Science Reviews, 8(4), 371–396.

Huppert, H. E. (1971). On the stability of a series of double-diffusive layers. Deep Sea Research and Oceanographic Abstracts, 18(10),1005–1021.

Huppert, H. E., and Turner, J. S. (1981). Double-diffusive convection. Journal of Fluid Mechanics, 106(-1), 299.

Jackson, M.P., Hudec, M.R., 2017. Salt Tectonics: Principles and Practice. Cambridge University Press.

Kirkham, C., Bertoni, C., Cartwright J., Lensky N.G., Sirota, I., Rodriguez, K. and Hodgson, N. (2020). The demise of a 'salt giant' driven by uplift and thermal dissolution. Earth and Planetary Science Letters. 531

Kostachuk, R., M.M. Nasr-Azadani, E. Meiburg, T. Wei, Z. Chen, M.E. Negretti, J. Best, J. Peakall and D.R. Parsons 2018 On the Causes of Pulsing in Continuous Turbidity Currents, J. Geophys. Res.: Earth Surface 123

Lensky, N.G., Dvorkin, Y., Lyakhovsky, V., Gertman, I. and Gavrieli, I. (2005) Water, salt, and energy balances of the Dead Sea. Water Resour. Res., 41, 1–13.

Lensky N., Gertman I., Rosentraub Z., Lensky I., Gavrieli I., Calvo R. and Katz O. (2010). Alternative dumping sites in the Dead Sea for harvested salt from pond 5: Final report. Geol. Surv. Israel, Rep. no. GSI/05/2010, 36 p.

Lensky N., Gertman I., Gavrieli I. (2011a). The expected quality of the Dead Sea brine expected to be pumped in the planned pumping station P9: Report A -Hydrography and the path of the industrial end brines in the Dead Sea. Geol. Surv. Israel, Rep. no. GSI/17/2011, 59 p.

Lensky N., Gertman I., Rosentraub Z., Lensky I., Nehorai R., Gavrieli I. (2011b). The expected quality of the Dead Sea brine expected to be pumped in the planned pumping station P9: Report B - Currents and transport of suspended matter. Geol. Surv. Israel, Rep. no. GSI/18/2011, 60 p.

Lensky N., Bodzin R., Arnon A., Gavrieli I. (2011c). The expected quality of the Dead Sea brine expected to be pumped in the planned pumping station P9: Report C - The salt delta. Geol. Surv. Israel, Rep. no. GSI/19/2011, 26 p.

Lensky, N. G., I. Gertman, A. Arnon, T. Ozer, E. Biton, B. Katsenelson, and R. Bodzin. (2013). Currents and hydrography of the Dead Sea: A study for the Salt Recovery Project. Geol. Surv. Israel Rep. no. GSI/20/2013, 31 p.

Lensky N.G., Lensky I.M., Peretz A., Gertman I., Tanny J., Assouline S. (2018). Diurnal course of evaporation from the Dead Sea in summer: a distinct double peak induced by solar radiation and night sea breeze. Water Resour. Res. 54

Linden, P. (1971). Salt fingers in the presence of grid-generated turbulence. Journal of Fluid Mechanics, 49(03), 611.

Linden, P. (1973). On the structure of salt fingers. Deep Sea Research and Oceanographic Abstracts, 20(4), 325–340.

Longuet-Higgins, M. S. (1970). Longshore currents generated by obliquely incident sea waves: 1. Journal of Geophysical Research, 75(33), 6778–6789.

Lowenstein, T.K., and Hardie, L.A., 1985, Criteria for the recognition of salt-pan evaporites: Sedimentology, v. 32, p. 627–644

Masselink, G. (1992). Longshore variation of grain size distribution along the Coast of the Rhone Delta, Southern France: A test of the McLaren Model. J. Coast. Res., 286–291.

Masselink, G., Hughes, M., and Knight, J. (2014). Introduction to coastal processes and geomorphology. Routledge.

McLaren, P., and Bowles, D. (1985). The effects of sediment transport on grain-size distributions. Journal of Sedimentary Research, 55(4), 457–470.

Meijer, P., Krijgsman, W. (2005). A quantitative analysis of the desiccation and refilling of the Mediterranean during the Messinian Salinity Crisis. Earth and Planetary Science Letters, 240(2), 510–520. https://doi.org/10.1016/j.epsl.2005.09.029

Mor Z., Assouline S., Tanny J., Lensky I.M., Lensky N.G. (2018). Effect of water surface salinity on evaporation: The case of a diluted buoyant plume over the Dead Sea. Water Resour. Res., 54

Mor, Z., Shalev, E., Lutzky, H., Lensky N.G. (2021) Density-depth profiler resolved by an array of pressure transducers and hydrostatic relations. Water, 13

Neev D, Emery K O. (1967). The Dead Sea: Depositional Processes and Environments of Evaporites. State of Israel, Ministry of Development, Geological Survey, Jerusalem. 147p.

Nehorai, R., I. M. Lensky, L. Hochman, I. Gertman, S. Brenner, A. Muskin, and N.G. Lensky (2013), Satellite observations of turbidity in the Dead Sea, J. Geophys. Res. Oceans, 118, 3146–3160

Newman , F.C., (1976). Temperature steps in Lake Kivu: a bottom heated saline lake. Journal of Physical Oceanography, 6(2), pp.157-163.

Oren A (2015) Limnological instrumentation in the middle of the 19th century: the first temperature and density profiles measured in the Dead Sea. Chinese Journal of Oceanology and Limnology, 33, 1496-1504

Ouillon, R., Lensky, N.G., Lyakhovsky, V., Arnon, A. and Meiburg, E. (2019a) Halite precipitation from double-diffusive salt fingers in the Dead Sea: Numerical simulations. Water Resour. Res., 55, 4252–4265.

Ouillon, R., N.T. Ouellette, J.R. Koseff and Meiburg (2019b) Interaction of a Downslope Gravity Current with an Internal Wave, J. Fluid Mech. 873, 889-913.

Radko, T. (2003). A mechanism for layer formation in a double-diffusive fluid. Journal of Fluid Mechanics, 497(497), 365–380.

Radko, T. (2013). Double-diffusive convection. Cambridge University Press, 2013. Cambridge University Press.

Roveri, M., Flecker, R., Krijgsman, W., Lofi, J., Lugli, S., Manzi, V., Sierro, F.J., Bertini, A., Camerlenghi, A., DeLange, G., Govers, R., Hilgen, F.J., Hubscher, C., Meijer, P.T. and Stoica, M. (2014a) The Messinian Salinity Crisis: Past and future of a great challenge for marine sciences. Mar. Geol., 352, 25–58.

Roveri, M., Manzi, V., Bergamasco, A., Falcieri, F.M., Gennari, R., Lugli, S., and Schreiber, B.C., 2014b, Dense shelf water cascading and messinian canyons: A new scenario for the mediterranean salinity crisis: American Journal of Science, v. 314, p. 751–784.

Schmalz, R. F. (1969). Deep-water evaporite deposition: A genetic model. AAPG Bulletin, 53(4), 798–823.

Schmitt, R. W. (1981). Form of the temperature-salinity relationship in the central water: Evidence for double-diffusive mixing. Journal of Physical Oceanography, 11(7), 1015–1026.

Schuch, F.N., Meiburg, E. and Silvestrini, J.H. 2021 Plunging Criterion for Particle-laden Flows over Sloping Bottoms: Three-dimensional Turbulence-resolving Simulations, Comp. and Geosci. 156, 104880.

Schumm SA and Khan HR. (1972). Experimental study of channel patterns. Geological Society of America Bulletin 83(6): 1755–1770.

Shields A. (1936). Application of Similarity Principles and Turbulence Research to Bed-Load Movement. Mitt. Preuss. Versuchsanst. Wasserbau Schiffbau 26: 47.

Simon, D., Meijer, P. T. (2017). Salinity stratification of the Mediterranean Sea during the Messinian crisis: A first model analysis. Earth and Planetary Science Letters, 479, 366–376.

Sirkes, Z., F. Schirmer, H. H. Essen, and K. W. Gurgel. (1997). Surface currents and seiches in the Dead Sea, p. 104–113. In T. M. Niemi, Z. Ben-Avraham, and J. R. Gat [eds.], The Dead Sea—the Lake and its setting. Oxford Univ. Press.

Sirota I., Arnon A., Lensky N.G. (2016). Seasonal variations of halite saturation in the Dead Sea. Water Resour. Res., 52

Sirota I., Enzel Y., Lensky N.G. (2017). Temperature seasonality control modern halite layers in the Dead Sea: In situ observations. Geol. Soc. Am. Bull., 129

Sirota I., Enzel Y., Lensky N.G. (2018) Halite focusing and amplifying salt-layer accretion: From the Dead Sea to deep hypersaline basins. Geology, 46.

Sirota, I., Ouillon, R., Mor, Z., Meiburg, E., Enzel, Y., Arnon. A., Lensky, N.G. (2020) Hydroclimatic Controls on Salt Fluxes and Halite Deposition in the Dead Sea and the Shaping of "Salt Giants". Geophysical Research Letters, 47.

Sirota, I., Enzel, Y., Mor, Z., Ben Moshe, L., Eyal, H., Lowenstein, T.K., Lensky, N.G. (2021) Sedimentology and stratigraphy of a modern halite sequence formed under Dead Sea level fall. Sedimentology, 68, 1069–1090.

Sirota, I., Armon, M., Ben Dor, Y., Morin, E., Lensky, N.G. and Enzel, Y., (2023). A mechanistic approach for interpreting hydroclimate from halite-bearing sediments. Sedimentology, 70(7), pp.2037-2056.

Stellmach, S., Traxler, A., Garaud, P., Brummell, N., Radko, T. (2011). Dynamics of fingering convection. Part 2 the formation of thermohaline staircases. Journal of Fluid Mechanics, 677, 554–571.

Steinhorn, I., Assaf, G., Gat, J.R., Nishry, A., Nissenbaum, A., Stiller, M., Beyth, M., Neev, D., Garber, R., Friedman, G.M. and Weiss, W. (1979) The dead sea: deepening of the mixolimnion signifies the overture to overturn of the water column. Science, 80, 55–57.

Steinhorn, I. (1983) In situ salt precipitation at the Dead Sea. Limnol. Oceanogr., 28, 580–583.

Steinhorn, I. (1985). The disappearance of the long term meromictic stratification of the Dead Sea. Limnology and Oceanography, 30(3), 451–472.

Stevens, C. L. and Lawrence, G. A. (1998) Stability and meromixis in a water-filled mine pit. Limnology and Oceanography, 43(5), 946–954.

Stern, M. E. (1960). The "Salt-Fountain" and Thermohaline Convection. Tellus, 12(2), 172–175.

Stern, M.E. and Turner, J.S. 1969 Salt fingers and convecting layers. Deep Sea Research and Oceanographic Abstracts 16, 497.

Stern, M. E., Radko, T. and Simeonov, J. 2001 3D salt fingers in an unbounded thermocline with application to the Central Ocean. J. Mar. Res. 59, 355–390

Stiller, M., J. R. Gat, N. Bauman, and S. Shasha. (1984). A short meromictic episode in theDead Sea: 1979–1982. SIL Proc. 1922–2010, 22: 132–135.

Stiller, M., J. R. Gat, and P. Kaushansky (1997), Halite precipitation and sediment deposition as measured in sediment traps deployed in the Dead Sea: 1981–1983, in The Dead Sea: The Lake and its Settings, edited by T. M. Niemi, Z. Ben-Avraham, and J. R. Gat, pp. 161–170, Oxford Univ. Press, Oxford.

Sutherland, B.R. 2010 Internal Gravity Waves, Cambridge University Press.

Törnqvist TE, Wortman SR, Mateo ZRP, Milne GA, Swenson JB. (2006). Did the last sea level lowstand always lead to cross-shelf valley formation and source-to-sink sediment flux? Journal of Geophysical Research: Earth Surface 111: 1–13.

Traxler, A., Stellmach, S., Garaud, P., Radko, T., Brummell, N. (2011). Dynamics of fingering convection. Part 1 Small-scale fluxes and large-scale instabilities. Journal of Fluid Mechanics, 677, 530–553.

Turner, J. (1967). Salt fingers across a density interface. Deep Sea Research and Oceanographic Abstracts, 14(5), 599–611.

Turner, J. S. (1974). Double-diffusive phenomena. Ann. Rev. of Fluid Mech., 6, 37–54.

Vachtman D, Laronne JB. (2013). Hydraulic geometry of cohesive channels undergoing base level drop. Geomorphology, 197, 76-84.

Van Hijum, E., and Pilarczyk, K. W. (1982). Gravel beaches: Equilibrium profile and longshore transport of coarse material under regular and irregular wave attack. Hydr. lab.

von Rohden, C., Boehrer, B., and Imberger, J. (2010). Evidence for double diffusion in temperate meromictic lakes. Hydrology and Earth System Sciences, 14(4), 667–674.

Vowinckel, B., J. Withers and P. Luzzatto-Fegiz 2019 Settling of Cohesive Sediment: Particle-Resolved Simulations, J. Fluid Mech. 858, 5-44.

Warren, J., 1999. Evaporites: Their Evolution and Economics. Blackwell Science, Oxford.

Warren, J. K. (2010). Evaporites through time: Tectonic, climatic and eustatic controls in marine and nonmarine deposits. Earth-Science Reviews, 98(3–4), 217–268.

Weinstein, R., N. Paldor, D. A. Anati, and A. Hecht. (2000). Internal seiches in the strongly stratified Dead Sea. Isr. J. Earth Sci. 49: 45–53.

Weisbrod N. Yechieli Y, Shandalov S., Lensky N. (2016). On the Viscosity of Natural Highly-Saline Solutions and its Importance: The Dead Sea Brines as an Example. J. of Hydrology, 532.

Woolfe KJ, Larcombe P, Naish T, Purdon RG. (1998). Lowstand rivers need not incise the shelf: An example from the Great Barrier Reef, Australia, with implications for sequence stratigraphic models. Geology 26: 75–78.

Wüest, A., Aeschbach-Hertig,W., Baur, H., Hofer, M., Kipfer, R., and Schurter, M. (1992). Density structure and tritium-helium age of deep hypolimnetic water in the northern basin of Lake Lugano. Aquatic Sciences, 54(3-4), 205–218.

Zodiatis, G., & Gasparini, G. Pietro. (1996). Thermohaline staircase formations in the Tyrrhenian Sea. Deep-Sea Research Part I: Oceanographic Research Papers, 43(5), 655–678.